THE JOURNAL OF BIOLOGICAL CHEMISTRY VOL. 282, NO. 52, pp. 37350–37358, December 28, 2007

Extracellular ATP Mediates Necrotic Cell Swelling in SN4741 Dopaminergic Neurons through $P2X_7$ Receptors*[S]

Received for publication, September 21, 2007, and in revised form, October 16, 2007 Published, JBC Papers in Press, October 25, 2007, DOI 10.1074/jbc.M707915200

Dong-Jae Jun[‡], Jaeyoon Kim[‡], Sang-Yong Jung[‡], Ran Song[‡], Ji-Hyun Noh[§], Yong-Soo Park[‡], Sung-Ho Ryu[‡], Joung-Hun Kim[‡], Young-Yun Kong[‡], Jun-Mo Chung[§], and Kyong-Tai Kim[‡1]

From the [‡]Department of Life Science, Division of Molecular and Life Science, Pohang University of Science and Technology, San-31, Hyoja-Dong, Nam-Gu, Pohang 790-784, Republic of Korea and the [§]Department of Life Sciences, College of Natural Sciences, Ewha Womans University, 11-1 Daehyun-Dong, Seodaemun-Gu, Seoul 20-750, Republic of Korea

Extracellular ATP has recently been identified as an important regulator of cell death in response to pathological insults. When SN4741 cells, which are dopaminergic neurons derived from the substantia nigra of transgenic mouse embryos, are exposed to ATP, cell death occurs. This cell death is associated with prominent cell swelling, loss of ER integrity, the formation of many large cytoplasmic vacuoles, and subsequent cytolysis and DNA release. In addition, the cleavage of caspase-3, a hallmark of apoptosis, is induced by ATP treatment. However, caspase inhibitors do not overcome ATP-induced cell death, indicating that both necrosis and apoptosis are associated with ATP-induced cell death and suggesting that a necrotic event might override the apoptotic process. In this study we also found that $P2X_7$ receptors ($P2X_7Rs$) are abundantly expressed in SN4741 cells, and both ATP-induced swelling and cell death are reversed by pretreatment with the $P2X_7Rs$ antagonist, KN62, or by knock-down of $P2X_7Rs$ with small interfering RNAs. Therefore, extracellular ATP release from injured tissues may act as an accelerating factor in necrotic SN4741 dopaminergic cell death via $P2X_7Rs$.

Parkinson disease (PD)[2] is an idiopathic neurodegenerative disorder characterized by selective cell death of dopaminergic neurons in the substantia nigra (1). The symptoms of PD only become apparent when more than 50% of the dopaminergic neurons in the substantia nigra *pars compacta* are lost, which leads to an over 80% reduction in dopamine levels in the striatum (2). Epidemiological studies and pathological analyses demonstrate that sporadic PD with late onset occurs in 95% of patients, whereas the remaining 5% of PD cases are familial diseases with early onset (1, 2). Although the etiological causes of PD have not been fully elucidated, several factors have been suggested as causes of neuronal degeneration. These include environmental toxins, genetic factors, and mitochondrial dysfunction as well as proteasomal impairment and oxidative stress (3). Recently, however, there has been increasing recognition of the possible role of neuro-inflammation as a major factor in the pathogenesis of PD (4). The inflammatory component is an attractive target for therapeutic intervention. It is now generally accepted that high levels of extracellular ATP may be released under pathological conditions such as inflammation, trauma, and stress. The role of extracellular ATP and purinergic receptors in neurodegeneration is one of the focus areas of cell death research (5).

$P2X_7$ receptors ($P2X_7Rs$) are unusual purinergic receptors in that they can exist in two functional states: either as cation-selective channels or as nonselective pores (6). The permeability transition of $P2X_7Rs$ from channel to pore occurs either upon sustained stimulation with high ATP concentrations or repeated pulses of ATP application (7). Seven members of the P2X receptor family have been cloned that share the same predicted structure with two transmembrane-spanning domains. These are an extracellular loop and the intracellular N- and C-terminal tails. Unlike other P2X receptor subtypes, $P2X_7R$ has an unusually long C-terminal domain that is responsible for the pore-forming property of $P2X_7Rs$ (8, 9). In addition, $P2X_7R$ does not hetero-oligomerize with other members of the P2X family but functions only in the homo-oligomeric form (10), most likely as a homotrimer.

Activation of this receptor also has dramatic cytotoxic properties that together with its ability to regulate cytokine production and release suggests that it can act as an important regulator of cell death in response to pathological insults (11). In most cells that express $P2X_7Rs$, sustained stimulation with ATP leads to membrane blebbing and programmed cell death. However, recent studies have shown that activation of $P2X_7Rs$ is involved in necrotic cell death as well as apoptosis. In murine thymocytes, ATP-mediated $P2X_7Rs$ activation leads to death via both caspase-dependent apoptosis and necrosis/lysis, even though necrotic cell death is predominant (12). In microglial N13 cells, inhibitors of caspases specifically suppress DNA fragmentation and other morphological signs of apoptotic damage. In con-

* This work was supported by Brain Neurobiology Research Program Grant M10412000023-06N1200-02310 and Korea Science and Engineering Foundation Grant R15-2004-033-06001-0 funded by the Korea government (Ministry of Science and Technology). This work was also supported by the Brain Korea 21 Program of the Korean Ministry of Education. The costs of publication of this article were defrayed in part by the payment of page charges. This article must therefore be hereby marked "*advertisement*" in accordance with 18 U.S.C. Section 1734 solely to indicate this fact.

[S] The on-line version of this article (available at http://www.jbc.org) contains supplemental Figs. S1–S5.

[1] To whom correspondence should be addressed: Dept. of Life Science, POSTECH, San-31, Hyoja-Dong, Nam-Gu, Pohang 790-784, Republic of Korea. Tel.: 82-54-279-2297; Fax: 82-54-279-2199; E-mail: ktk@postech.ac.kr.

[2] The abbreviations used are: PD, Parkinson disease; siRNA, small interfering RNA; $P2X_7R$, $P2X_7$ receptor; AM, acetoxymethyl ester; FACS, fluorescence-activated cell sorter; PI, propidium iodide; FITC, fluorescein isothiocyanate; RT, reverse transcription; MTT, 3-(4,5-dimethylthiazol-2-yl)-2,5-diphenyltetrazolium bromide; ER, endoplasmic reticulum; HEK, human embryonic kidney; ATPγS, adenosine 5′-*O*-(thiotriphosphate).

trast, cytoplasmic vacuolization and cell lysis remain unaffected, and cell death proceeds regardless of caspase activation (13). Necrotic cell death is usually accompanied by cell swelling, termed necrotic volume increase, whereas cell shrinkage is a major hallmark of apoptosis (14, 15). The acute excitotoxicity is thought to be mediated by excess depolarization of the postsynaptic membrane. This results in an osmotic imbalance caused by an influx of Na^+, Cl^-, and water, leading to cell lysis (16).

Recent studies have shown that $P2X_7$Rs are expressed in the mossy fibers of the CA3 area of the hippocampus (17), as well as in cultured astrocytes, Schwann cells (18), spinal cord neurons (19), and immune cells or microglia. Depending on the cell type, various physiological functions have been attributed to $P2X_7$Rs, most notably, activation of caspase-1 (20), rapid release of mature interleukin-1β from macrophages (21), shedding of membrane molecules such as L-selectin and CD23 (22), synaptic transmission in the hippocampus (19), and programmed cell death in injured spinal cords (23). However, the expression of $P2X_7$Rs and their functional role in the dopaminergic neurons, which are selectively degenerated in PD, has remained unexplored. In this study, we report that extracellular ATP induces cell death through $P2X_7$Rs in SN4741 cells, which are derived from substantia nigra dopaminergic neurons of transgenic mouse embryos (24). The ATP-induced cell death has similar responses to necrosis rather than apoptosis in SN4741 neurons. Thus, $P2X_7$Rs may be involved in degeneration of substantia nigra dopaminergic neuron according to the progression of Parkinson disease through an association with necrotic volume increase.

EXPERIMENTAL PROCEDURES

SN4741 Dopaminergic Cell Culture—SN4741, a mouse embryonic substantia nigra-derived cell line, was grown at 33 °C in a 5% CO_2-humidified atmosphere in Dulbecco's modified Eagle's high glucose medium (Invitrogen) containing 10% heat-inactivated calf serum (Hyclone; Logan, UT) and 1% (v/v) antibiotics (Invitrogen). The medium was changed every 2 days, and the cells were subcultured approximately twice a week.

Calcium Measurements—Intracellular Ca^{2+} concentration ($[Ca^{2+}]_i$) was determined using the fluorescent Ca^{2+} indicator, fura-2, as previously reported (25). Briefly, SN4741 cells were incubated with 3 μM (final concentration) fura-2 pentaacetoxymethyl ester (fura-2/AM) in complete medium at 37 °C with stirring for 50 min. After incubation, the cells were pelleted and washed twice with Locke's solution (154 mM NaCl, 5.6 mM KCl, 1.2 mM $MgCl_2$, 2.2 mM $CaCl_2$, 5.0 mM HEPES, 10 mM glucose, pH 7.4) to remove the extracellular dye. To prevent dye leakage, sulfinpyrazone (final concentration, 250 nM) was then added to both the loading medium and the washing solution, as previously described (26). Fluorescence ratios were taken by dual excitation at 340 and 380 nm, and the emission was measured at 500 nm with an alternative wavelength time scanning method. Calibration of the fluorescence signal, in terms of $[Ca^{2+}]_i$, was performed according to Grynkiewicz *et al.* (27).

Confocal Microscopy—To record fluorescence images, adipocytes cultured on poly-D-lysine-coated coverslips were preloaded with 5 μM Fluo-4/AM dye. After incubation for 30 min at 37 °C, the cells were washed two times in Locke's solution to remove excess dye and examined under the confocal microscope. Measurement of intracellular calcium was performed with the Bio-Rad Radiance 2100 confocal microscope equipped with a 40× objective and a 0.75 numerical aperture. The calcium-sensitive Fluo-4 dye was excited by the 488-nm line from an argon laser, and the emission fluorescence was monitored at 515 ± 15 nm and selected by a band pass filter. During the collection of fluorescence data, each scan of a 512 × 512-pixel image took 0.35 s, and the interval between each image scan was ~2 s. The images were stored and processed using laser pix software. The regions of interest, distributed across the image, provided an intensity *versus* time graphic output.

FACS Analysis—Following treatment of SN4741 cells with ATP for the indicated time, apoptotic cells and necrotic cells were analyzed by staining the cells with annexin V and propidium iodide (PI), in accordance with the manufacturer's instructions (BD Pharmingen apoptosis kit, San Diego, CA). Briefly, an aliquot of 10^5 cells was incubated with annexin V-fluorescein isothiocyanate (FITC) and PI for 15 min at room temperature in the dark. The cells were immediately analyzed by FACScalibur (Becton Dickinson, Heidelberg, Germany). The emission/excitation wavelengths were 530/488 nm for Annexin V FITC (FL1) and 650 nm/488 nm for PI (FL2), according to the manufacturer's specifications of wavelength combinations. The necrotic cells were annexin V- and PI-positive, whereas apoptotic cells were annexin V-positive and PI-negative. The percentage of cells stained in each quadrant was quantified using the CellQuest software (BD Biosciences, San Jose, CA). Cell volume changes were also measured using a FACScalibur flow cytometer, and CellQuest software was used for data analysis (28). The light scatter channels were set on linear gains. The cells in suspension, in Locke's solutions, were gated for forward angle scatters, and 20,000 particles of each gated population were analyzed. The cells were passed in single file through a laser beam by continuous flow of a fine stream of the suspension. Each cell scatters laser light, and the cytometer can simultaneously measure several typical parameters for each cell. These include flow angle and forward scatter intensity, which is proportional to the cell diameter.

RT-PCR Analysis—Total RNA was extracted from SN4741 cells by TRI reagent (Molecular Research Center, Cincinnati, OH). One microgram of total RNA was reverse-transcribed using Superscript II reverse transcriptase (Invitrogen). cDNA was amplified with 20 pmol of specific oligonucleotide primers (Bioneer) using Ex Taq polymerase (TaKaRa). The PCR products were analyzed on a 1% agarose gel and by sequencing. Nucleotide sequence analysis confirmed that the amplified DNA product from SN4741 cells was authentic mouse $P2X_7$Rs.

RNA Interference—siRNA duplexes targeting $P2X_7$R (5′-GCAGGUGUGUUCCAUAUGA-3′ and 5′-UCACCGUACUCAUCAAGAG-3′) were purchased from Dharmacon. Transfection with siRNA pools was performed by electroporation, and down-regulation of $P2X_7$R was confirmed by Western blot analysis.

Western Blot—Immunoblot analysis was performed as described previously (25). SN4741 cells were plated on 60-mm tissue culture dishes and transfected with siRNA targeting $P2X_7$R as indicated. After transfection, the cells were washed twice with cold phosphate-buffered saline and then lysed with lysis buffer

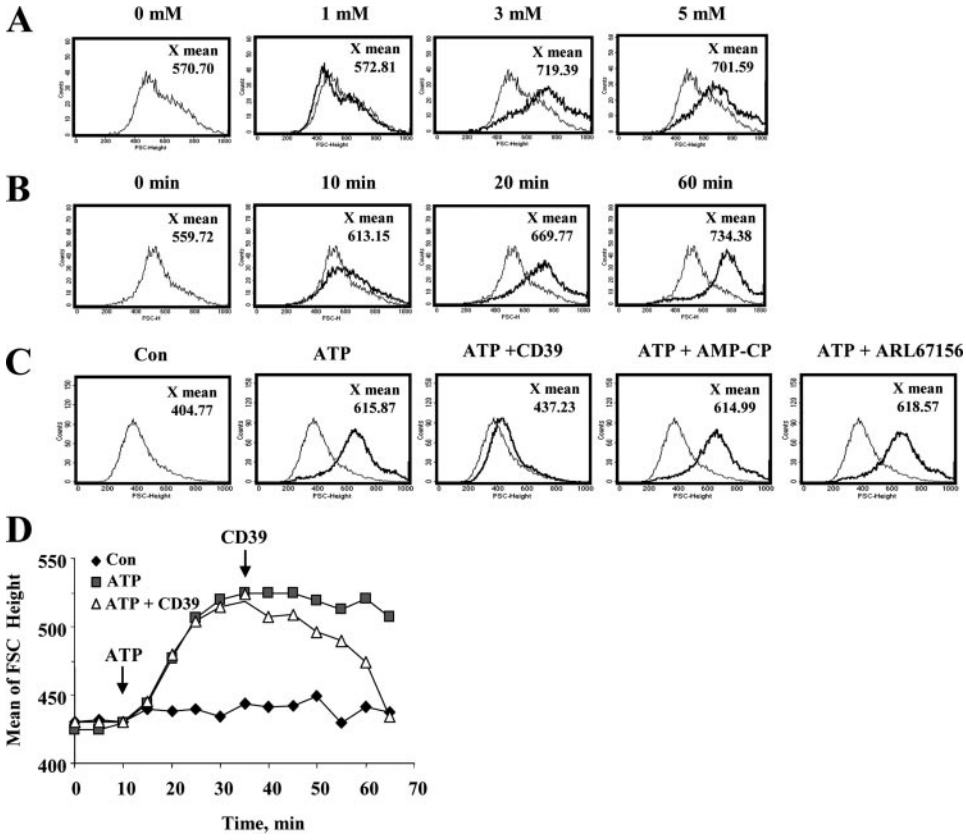

FIGURE 1. **Extracellular ATP induced SN4741 dopaminergic cell volume increase.** *A*, concentration-dependent response of ATP-induced volume increase in SN4741 cells. The cells were exposed to the indicated concentrations of ATP for 20 min. *B*, time course of ATP-induced volume increase in SN4741 cells. The cells were treated with 3 mM ATP for indicated times. *C*, ATP-induced volume increase was completely inhibited by a 5-min pretreatment with CD39 (20 units/ml), but not by AMP-CP (100 μM) and ARL67156 (100 μM). *D*, ATP-mediated volume increase became attenuated after treatment with CD39 (20 units/ml) at indicated time. Cell volume changes were examined by flow cytometry and analyzed by gating on a forward scatter histogram (cell size). The histograms are representative of three to four independent experiments. *Con*, control.

(250 mM Tris-Cl, pH 6.5, 2% SDS, 4% β-mercaptoethanol, 0.02% bromphenol blue, and 10% glycerol). Equivalent amounts of protein were resolved by SDS-PAGE and analyzed by Western blotting. The signals were detected with an ECL detection system (Neuronex Co.). The estimated size was 70 kDa in SN4741 cells, which is the appropriate molecular mass of the $P2X_7R$ subtype.

MTT Viability—Cell viability was assessed by measuring the ability of cells to metabolize MTT. The cells were seeded onto 96-well plates at a density of $\sim 2 \times 10^4$ cells/well in growth medium and cultured to ~60–70% confluency prior to the initiation of experimental treatment. Following the treatments as indicated, 15 μl of MTT solution (5 mg/ml) was added to each well, and the cells were maintained for 1 h at 37 °C. 100 μl of solubilizing solution (50% dimethylformamide and 20% SDS, pH 4.8) was then added. After an overnight incubation at room temperature, absorbance was measured at 570 nm.

Measurement of Intracellular Na^+ Levels—The level of intracellular Na^+ was determined as previously described using the SBFI/AM fluorescence sodium indicator (29). The cells were harvested and incubated in serum-free Dulbecco's modified Eagle's medium with 15 μM SBFI/AM, 0.2% pluronic acid, and 250 μM sulfinpyrazone at 37 °C for 90 min under continuous stirring. The cells were then washed with serum-free RPMI 1640 solution containing 250 μM sulfinpyrazone. Before measurement, a small aliquot of the cells (1×10^6 cells) was withdrawn, centrifuged, and resuspended in Locke's solution. In these experiments, the increase in cytosolic Na^+ was measured as an increase in the fluorescence ratio determined at the dual excitation wavelengths of 340 and 380 nm and the emission wavelength of 520 nm at 37 °C. The results are expressed as fluorescence ratios.

Electron Microscopy—SN4741 cells were stimulated and grown on Vitrogen collagen matrix (Cohesion, Palo Alto, CA). As we described previously (30), these cells were rinsed two times with phosphate-buffered saline and fixed with 2% paraformaldehyde and 2% glutaraldehyde in 50 mM sodium cacodylate buffer, pH 7.4, for 20 min at room temperature. The cells were subsequently postfixed with 0.5% osmium tetroxide in 0.05 M sodium cacodylate buffer, pH 7.4, for 30 min at room temperature. The cells were further dehydrated in graded ethanol solutions and embedded in LR White resin (London Resin Co., Berkshire, UK). The resin was cured at 60 °C for 24 h. Silver-gold thin sections were stained with uranyl acetate and lead citrate. The thin sections were examined under a JEOL 1200 EX2 transmission electron microscope at 80 kV (30).

Whole Cell Recordings—Whole cell recordings were made from coronal sections (250-μm thickness) containing the dopaminergic neurons of the substantia nigra *pars compacta* and performed using an axopatch 200A instrument (Axon Instruments). The slices were perfused (2 ml/min) with extracellular solution containing 130 mM NaCl, 24 mM $NaHCO_3$, 1.25 mM NaH_2PO_4, 2.5 mM $CaCl_2$, 2 mM $MgCl_2$, 10 mM glucose saturated with 95% O_2, 5% CO_2, pH 7.4: ATP, BzATP, and KN62 were added to the extracellular solution. The neurons were visually identified within 80-μm slices using infrared-differential interference contrast video microcopy (Leica), in a voltage clamp mode, at a holding potential of −60 mV. Recording electrodes (3–7 MΩ), pulled from borosilicate glass (World Precision Instruments (WPI, Inc), were filled with 150 mM cesium gluconate, 5 mM EGTA, 10 mM HEPES, 3 mM $MgCl_2$, adjusted to pH 7.2 with the addition of CsOH. All of the experiments were performed at room temperature (18–22 °C). Axon DigiData 1332A and pClamp 9.2 software (Axon Instruments) were used to acquire the data and for analysis.

Statistics—For statistical analysis, the paired Student's *t* test was used, and *p* values of less than 0.05 were regarded as significantly different.

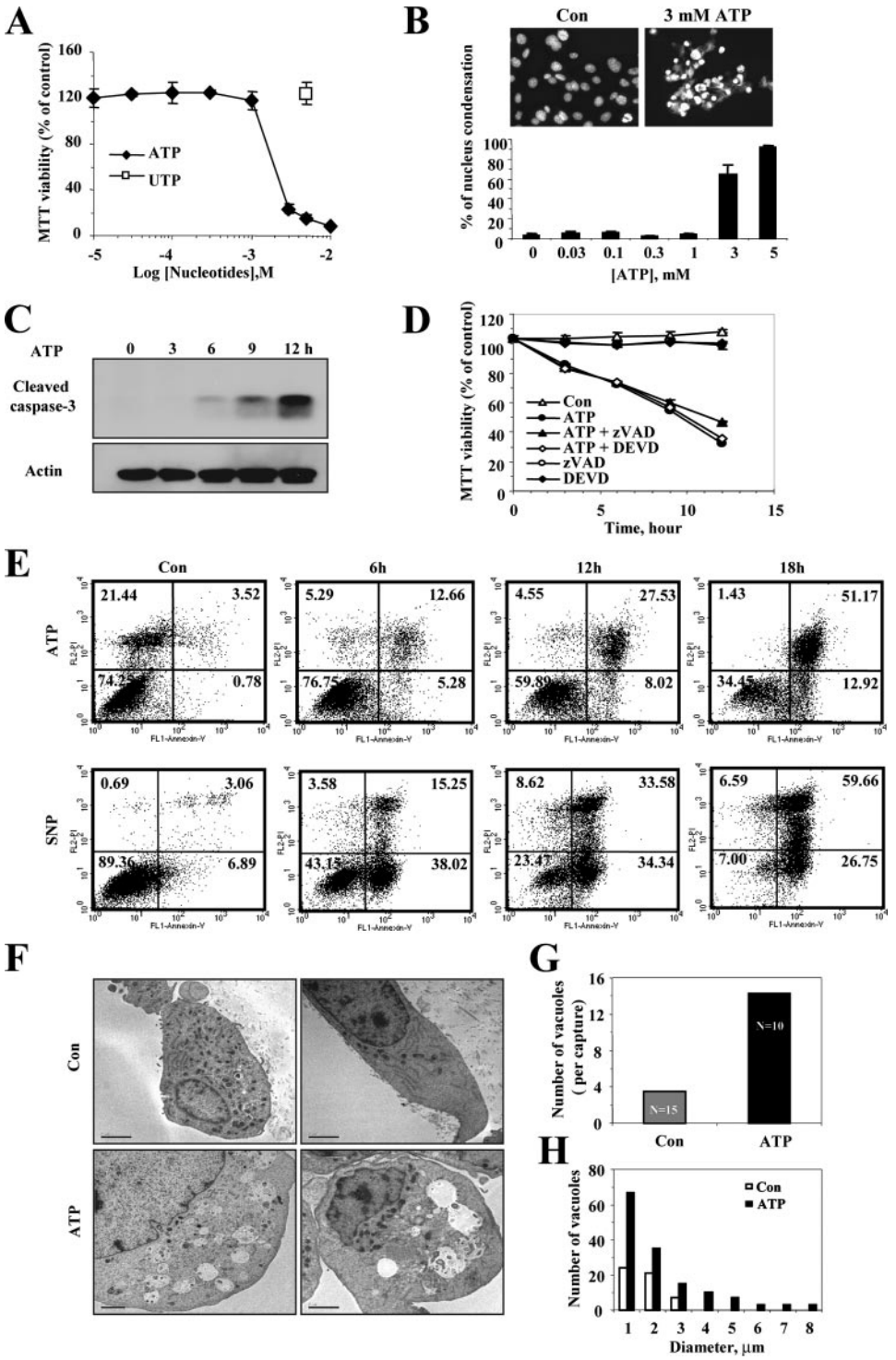

FIGURE 2. **Extracellular ATP induced necrosis in SN4741 dopaminergic neurons.** Concentration-dependent response of ATP-induced cell death in SN4741 cells is shown. The cells were exposed to the indicated concentrations of ATP or UTP for 12 h. *A*, the viability of the cells was determined by the MTT reduction assay and is expressed as a percentage of untreated control cells. Each point represents the mean ± S.D. of triplicates. *B*, the cells were fixed and stained with Hoechst dye 33342 (1 μg/ml), and nuclei were visualized by fluorescence microscopy (magnification, 400×). The cells with condensed nuclei were counted and are expressed as a percentage of untreated control cells. The photographs are representative of three experiments. Time course of ATP-induced cell death in SN4741 is shown. The cells were exposed to 3 mM ATP for the indicated periods of time. *C*, cells were harvested, lysed, and used for Western blot analysis with anti-cleaved caspase-3 antibody. *D*, pretreatment with caspase inhibitors did not affect ATP-induced cell death. The cells were exposed to 3 mM ATP for the indicated periods of time in the presence or absence of the pan-caspase inhibitor, zVAD-fmk (50 μM), or the specific caspase-3 and caspase-7 inhibitor, DEVD-CHO (50 μM). Cell viability was assessed by the MTT reduction assay and is expressed as a percentage of untreated control cells. Each point represents the mean ± S.D. of triplicates. *E*, extracellular ATP-induced necrotic cell death in SN4741 cells. Annexin V-FITC/propidium iodide staining of SN4741 cells was assessed by flow cytometry at indicated times after treatment. Sodium nitroprusside was used as a typical apoptosis-inducing reagent. Quadrants are defined as: live (*lower left*), apoptotic (*lower right*), and necrotic (*upper left* and *right*). The results are representative of three independent experiments. *F*, electron microscopic analysis of vehicle- and ATP-treated SN4741 cells. Typical morphological features of cells exposed to 3 mM ATP for 8 h were observed. Note the lack of ER integrity and the enhanced cytoplasmic swelling in ATP-treated cell. *G* and *H*, increases in both numbers and size of cytoplasmic vacuoles were observed in ATP-treated SN4741 cells. *Scale bars*, 2 μm. *Con*, control.

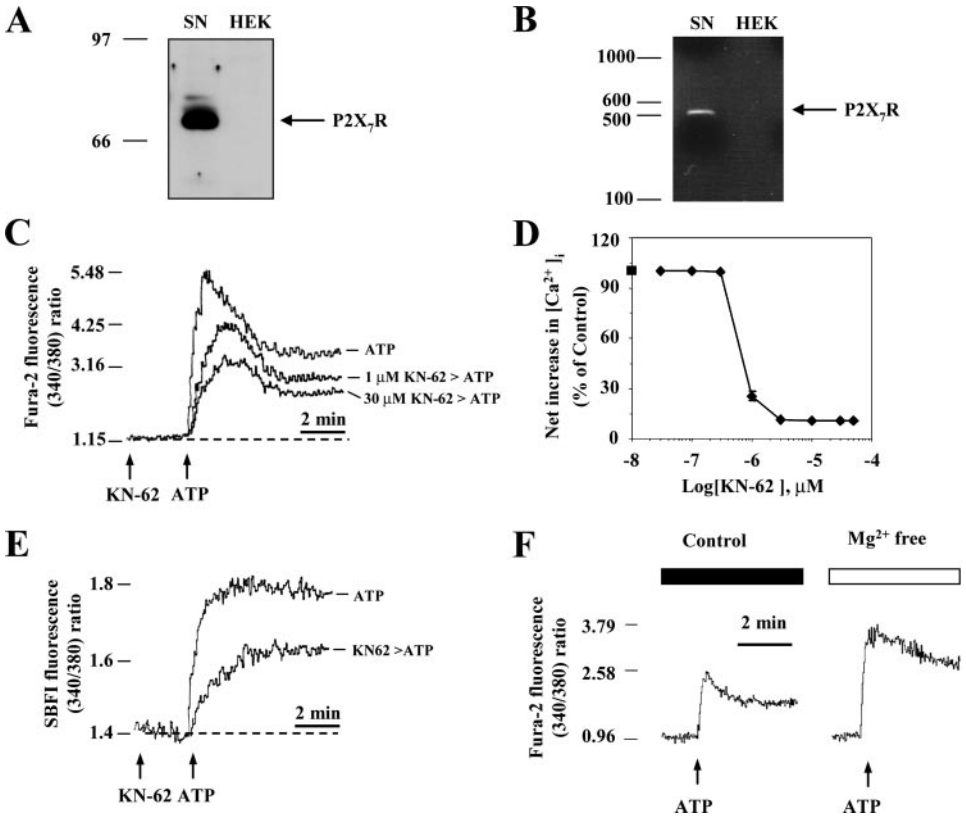

FIGURE 3. **SN4741 dopaminergic cells express functional $P2X_7Rs$.** *A*, immunoblot analysis of the $P2X_7Rs$ in SN4741 cells. A sample of total cell lysate (30 μg of protein) from SN4741 cells was run in parallel with a sample of HEK cell lysate (30 μg, negative control) and probed with $P2X_7Rs$ antibody. Size standards are shown in the *left lane*. *B*, expression of $P2X_7Rs$ mRNA in SN4741 cells. RT-PCR was performed on 1 μg of total RNA extracted from either SN4741 cells or HEK cells. Thirty-five PCR cycles were conducted with the same RT products using specific primers for $P2X_7Rs$. The products were analyzed by agarose gel electrophoresis. The size standards are shown in the *left lane*. *C*, ATP-induced influxes of Ca^{2+} were inhibited by KN-62, a specific P2X7 receptor antagonist. Ratiometric fluorescence measurement of fura-2/AM was performed in SN4741 cells. Application of KN-62 (30 μM) reduced ATP-induced influxes of Ca^{2+}. Typical Ca^{2+} traces are representative of four independent experiments. *D*, concentration-dependent effects of KN-62 on ATP-induced Ca^{2+} influx were assessed. SN4741 cells were pretreated with the indicated concentration of KN-62 for 2 min and then stimulated with 3 mM ATP. The experiments were performed three times, and each point is the mean ± S.D. *E*, ATP–induced influxes of Na^+ were inhibited by KN-62. Ratiometric fluorescence measurements of SBFI-AM were performed in SN4741 cells. Application of KN-62 (30 μM) reduced ATP-induced influxes of Na^+. Typical Na^+ traces are representative of four independent experiments. *F*, effect of Mg^{2+} in ATP-induced Ca^{2+} influx. SN4741 cells were stimulated with 300 μM ATP in the presence or absence of Mg^{2+}. The traces are representative of three independent experiments.

RESULTS

ATP-induced Volume Increase in SN4741 Cells—ATP-induced volume changes in SN4741 cells were assessed by flow cytometry. When SN4741 cells were exposed to millimolar concentrations of ATP, dramatic increases in cell volume were detected within 20 min in a concentration-dependent manner (Fig. 1, *A* and *B*). Under normal physiological conditions, extracellular ATP acts on P2 purinergic receptors in the plasma membrane. However, many cells express ecto-ATPases and CD39 (ecto-ATP diphosphohydrolase), which rapidly hydrolyze ATP into AMP on their plasma membranes. The AMP is subsequently hydrolyzed by 5-nucleotidase to generate adenosines, which acts as ligand for P1 purinergic receptors (6). To test whether the ATP-induced volume increase is related to this metabolic conversion of ATP, the changes in cell volume were checked in the presence of the ecto-ATPase inhibitor ARL67156, the 5-nucleotidase inhibitor AMP-CP, and CD39, which metabolizes ATP and ADP to AMP (31). This experiment showed that ATP-induced cell swelling was completely blocked by pretreatment with CD39, but it was unaffected by AMP-CP and ARL67156 (Fig. 1*C*). Furthermore, the cell swelling was immediately reversed after the addition of CD39 (Fig. 1*D*). These results indicate that cell swelling in SN4741 cells as a direct result of ATP and not of its metabolic intermediates such as ADP, AMP, and adenosine.

ATP-induced Necrotic Cell Death of SN4741 Cells—Because the dramatic volume increase by ATP stimulation may lead to cell death, we tested cell viability after ATP stimulation using MTT assays. ATP treatment for 12 h resulted in a concentration-dependent decrease in the viability of SN4741 cells, whereas treatment with UTP did not trigger the cell death (Fig. 2*A*). In addition, the changes in nuclear morphology were observed using Hoechst staining, which is used to identify apoptotic nuclei by the appearance of blue-colored apoptotic bodies present as peripherally clumped or fragmented chromatin in cells (32). Interestingly, however, the Hoechst staining results exhibited cytolysis and subsequent DNA release from nucleus into cytosol rather than apoptotic bodies (Fig. 2*B*). These morphological changes were visible at concentrations as high as 3 mM ATP in SN4741 cells. ATP stimulation also induced the cleavage of caspase-3, a hallmark of apoptosis, by ATP stimulation (Fig. 2*C*). However, caspase inhibitors, such as zVAD and DEVD, did not block the ATP-induced cell death (Fig. 2*D*). These results imply that ATP-induced cell death in SN4741 cells was associated with both necrosis and apoptosis, but necrotic events overrode apoptotic events. For precise differentiation between cells undergoing necrosis or apoptosis in the ATP-mediated cell death, the staining pattern of the cells were analyzed with PI and fluorochrome-conjugated annexin V by flow cytometry. Because cell undergoing apoptosis expose phosphatidylserine on their outer plasma membrane in the early processes and lose membrane integrity in the late processes, apoptotic cells are stained with annexin V-FITC, but not with PI. In contrast, because cells undergoing necrosis exhibit both phosphatidylserine exposure and loss of membrane integrity simultaneously, necrotic cells are stained with both PI and annexin V-FITC (4). In this experiment, SN4741 cells stimulated with ATP were stained simultaneously with both annexin V-FITC and PI (Fig. 2*E*), whereas SN4741 cells stimulated with

the NO donor sodium nitroprusside as an apoptosis-inducing reagent initially showed phosphatidylserine exposure and, ultimately, PI staining, is quite a different pattern compared with ATP-treated cells. Morphological characteristics visible at the electron microscope level have been accepted as reliable criteria to differentiate between necrosis and apoptosis, because necrosis results in early cell swelling, dilation of the Golgi apparatus and of the endoplasmic reticulum (ER), and loss of plasma membrane integrity (33). In our study, electron microscopy also provided a clear indication that necrosis had taken place. SN4741 cells displayed dramatic morphological changes accompanied by loss of ER integrity and formation of many large cytoplasmic vacuoles 8 h after ATP stimulation (Fig. 2, *F–H*). Taken together, these findings show that ATP-induced cell death is accompanied by cell swelling and suggests that cells are dying mainly by necrosis rather than apoptosis.

Functional Expression of P2X$_7$Rs in SN4741 Cells—P2X$_7$R activation was examined to determine whether it mediated ATP-induced cell swelling and subsequent cell death. To determine the expression of P2X$_7$Rs, we performed Western blot and RT-PCR analyses with total proteins and RNAs from SN4741 cells, respectively. For comparison, a human embryonic kidney (HEK) cell line was also tested that is known not to express P2X$_7$Rs (34). In these experiments, SN4741 cells, but not HEK cells, exhibited immunoreactivity with antibodies against P2X$_7$Rs and produce P2X$_7$R-specific DNA fragments with RT-PCR analysis (Fig. 3, *A* and *B*). To confirm the functionality of P2X$_7$Rs, we monitored ion flows such as Ca^{2+} and Na^+ upon ATP treatment, by using the ion-selective fura-2 or SBFI fluorescent indicator dyes. Stimulation of SN4741 cells with 100 μM ATP induced a modest and transient rise in $[Ca^{2+}]_i$ (supplemental Fig. S2*A*), which is likely because of activation of P2Y receptors (supplemental Fig. S2*C*). However, a strikingly different response was elicited when 3 mM ATP was added to SN4741 cells (Fig. 3*C*). Under these conditions, the Ca^{2+} peak was 2–3-fold higher, and the fast initial rise of Ca^{2+} was followed by a very slow decrease (sustained plateau). To assess whether the ATP-induced calcium increase was mediated by P2X$_7$Rs, we used an isoquinoline sulfonamide derivative, KN-62, which is known to be a potent inhibitor of P2X$_7$Rs (35). As shown in Fig. 3*C*, preincubation of SN4741 cells with KN-62 reduced the ATP-elicited Ca^{2+} response in a concentration-dependent manner. Effective KN-62 concentrations ranged between 0.3 and 3.0 μM with a maximal effective concentration of 3 μM (Fig. 3*D*). In addition, various nucleotides and ATP analogs increased $[Ca^{2+}]_i$ in SN4741 cells with the following rank order of potency: BzATP > ATP > ATPγS > ADP > 2MeSATP (supplemental Fig. S2). These results show characteristic features of P2X$_7$Rs expression in SN4741 cells. Extracellular ATP also stimulated a fast and long lasting Na^+ influx that was also reduced by pretreatment with KN-62 (Fig. 3*E*). It is generally recognized that the active form of ATP on P2X$_7$Rs is the free tetraionic form (ATP^{4-}). The addition of divalent cations decreases the concentration of the active tetraionic form (36). Therefore, depletion of Mg^{2+} in Locke's solution would be expected to enhance the ATP response in SN4741 cells. As expected, when cells were exposed to ATP in Mg^{2+}-free Locke's solution, both the Ca^{2+} peak and the sustained plateau

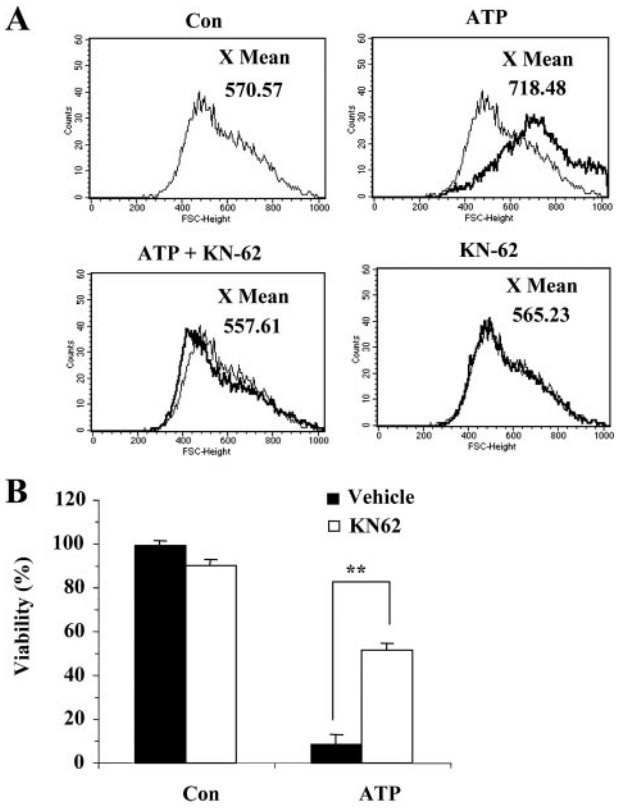

FIGURE 4. **Antagonist of P2X$_7$Rs blocks ATP-induced volume increase and cell death.** *A*, the ATP-induced volume increase was blocked by KN-62. SN4741 cells were pretreated with KN-62 (30 μM) for 1 min before and after ATP (3 mM) stimulation for 20 min. The volume increase was evaluated by FACS analysis. The results are representative of three independent experiments. *B*, pretreatment with KN-62 inhibited ATP-induced cell death. The cells were incubated with ATP (3 mM) for 12 h in the presence or absence of KN-62 (30 μM). Cell viability was assessed by the MTT reduction assay and is expressed as a percentage of untreated control cells. Each point represents the mean ± S.D. of triplicates. *Con*, control.

were enhanced (Fig. 3*F*). Other effects mediated by P2X$_7$Rs, such as membrane blebbing (37) and irreversible inhibitory effects of oxidized ATP (38), were also observed in SN4741 cells upon ATP stimulation (supplemental Figs. S1 and S3). Finally, the whole cell patch clamp technique was also used to detect inward currents by application of BzATP or ATP to mouse brain slices containing dopaminergic neurons in the substantia nigra *pars compacta*; furthermore these inward currents were suppressed by KN-62 (supplemental Fig. S4). Taken together, these results suggest that SN4741 dopaminergic cells express functionally active P2X$_7$Rs.

Involvement of P2X$_7$Rs in ATP-induced Cell Death and Volume Increase—To determine whether both ATP-induced cell death and volume increase are mediated by P2X$_7$Rs, SN4741 cells were preincubated with KN-62, and then changes in cell viability and volume increase were measured upon ATP stimulation. Preincubation of SN4741 cells with 1 μM KN-62 completely inhibited the 3 mM ATP-induced volume increase and, significantly, blocked more than 50% of the ATP-induced cell death. Preincubation with KN-62 alone affected neither cell volume nor viability of the cells (Fig. 4). To further verify the involvement of P2X$_7$Rs in ATP-induced cell death and volume increase, we used two different siRNAs (siP2X$_7$R 460 and siP2X$_7$R 574) to knock down endogenous P2X$_7$Rs. The effi-

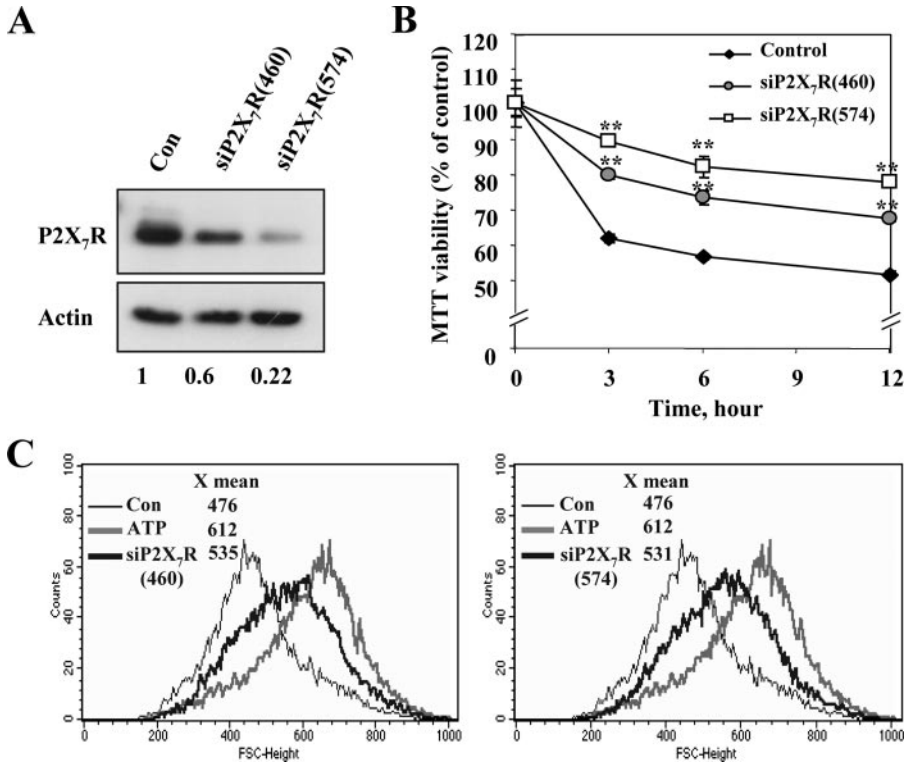

FIGURE 5. **Suppression of endogenous $P2X_7Rs$ expression attenuated ATP-induced cell death and volume increase.** SN4741 cells were transfected for 48 h with siRNAs that either specifically targeted $P2X_7Rs$ ($siP2X_7R$ (460), $siP2X_7R$ (574)), or served as a control (scrambled siRNA). *A*, the $P2X_7Rs$-specific siRNAs decreased endogenous $P2X_7Rs$ expression as detected by Western blotting using a $P2X_7Rs$-specific antibody. β-Actin served as an internal control (*bottom*). Densitometry measurement indicated that siRNAs (siP2X7 460 and siP2X7 574) decreased P2X7 expression levels by 40 and 78%, respectively, in comparison with basal levels. The picture shown is a representative of three independent experiments. *B*, time course of ATP-induced cell death transfected with the $P2X_7Rs$-specific siRNAs. $P2X_7Rs$ knock-down in SN4741 cells was stimulated with 3 mM ATP for the indicated periods of time. Cell viability was assessed by the MTT reduction assay and is expressed as a percentage of untreated cells. Each point represents the mean ± S.D. of triplicates. Significance is defined as $p < 0.001$ (**) relative to the respective control group. *C*, the $P2X_7R$-specific siRNAs decreased ATP-induced volume increase. $P2X_7R$ knock-down and volume increase, in cells incubated with 3 mM ATP for 20 min, was evaluated by FACS analysis. The results are representative of three independent experiments. *Con*, control.

ciency of knock-down by $siP2X_7Rs$ was evaluated by determining the $P2X_7R$ protein levels at 48 h after transfection. Endogenous $P2X_7R$ levels were knocked down with more than 50 and 80% efficiency by $siP2X_7R$ 460 and 574, respectively (Fig. 5*A*). The $siP2X_7Rs$ significantly improved the survival of SN4741 cells, up to 80% (Fig. 5*B*) and attenuated the ATP-induced volume increase by more than 70% (Fig. 5*C*). Recently, several loss-of-function polymorphisms affecting the human $P2X_7$ receptor have been identified (39–42). $P2X_7R$ carrying the R307Q mutation was reported to lack either channel or pore function because of the failure of ATP binding to the extracellular domain of $P2X_7R$ (39). In line with this, we also observed that HEK293 cells transfected with R307Q mutant $P2X_7R$ did not exhibit ATP-induced volume increase and cell death, but those transfected with wild type $P2X_7R$ did (supplemental Fig. S5). Together with the pharmacological data, these findings suggest that $P2X_7Rs$ play a key role in the ATP-induced dopaminergic cell volume increase and in cell death.

DISCUSSION

The present study has revealed, for the first time, that $P2X_7Rs$ are functionally expressed in SN4741 dopaminergic cells and that these receptors are responsible for ATP-induced cell swelling and necrotic cell death. There has been substantial controversy regarding the existence and function of neuronal $P2X_7Rs$ because currently antibodies against neuronal $P2X_7Rs$ are not highly specific (43, 44). However, this study shows that $P2X_7Rs$ are expressed in SN4741 dopaminergic neurons. The evidence is as follows: 1) RT-PCR analysis demonstrates that $P2X_7Rs$-specific DNA sequences are detected in SN4741 cells; 2) $P2X_7R$ gene knock-down experiments with specific siRNAs show a down-regulation of $P2X_7Rs$ expression, confirming the existence of $P2X_7Rs$; 3) pharmacological approaches using various nucleotides (Bz-ATP) and selective inhibitors (KN62 and oxidized ATP) correlate well with characteristics of $P2X_7Rs$; and 4) the inhibitory effect of extracellular Mg^{2+} on ATP-induced calcium influx and the ATP-stimulated appearance of membrane blebbing is consistent with the expression of typical $P2X_7Rs$.

This study also found that the main pathway of $P2X_7Rs$-mediated SN4741 cell death is by necrosis/lysis rather than apoptosis. ATP-treated cells revealed nuclear swelling and spill over of nuclear DNA to the extracellular space accompanied with morphological alterations including a loss of ER integrity and the formation of cytoplasmic vacuoles. These findings were further supported by demonstrating that ATP treatment simultaneously increases both the phosphatidylserine exposure and the PI staining in SN4741 cells, which is consistent with typical necrotic cell death.

It is noteworthy that ATP treatment also induces cleavage of caspase-3, one of the indicators of apoptosis. However, ATP-induced cell death was not affected by caspase inhibitors such as zVAD and DEVD. This result indicates that necrosis was the predominant mechanism by which ATP-induced cell death occurs, even though $P2X_7R$ activation can lead to both apoptosis and necrosis. This result is in line with a previous report showing that inhibition of caspase activity by zVAD has no significant effect on $P2X_7R$-mediated changes in cytoplasmic cell morphology, cell swelling, and cytoplasmic vacuolization in the thymocytes (12) and the N13 mouse glial cell line (13).

Apoptosis and necrosis have long been considered to be two distinct mechanisms of cell death, with different biochemical, morphological, and functional characteristics. However, recently it has become widely accepted that apoptosis and necrosis may not necessarily be independent pathways but

rather may share some common events, at least in some signal transduction pathways and in the early phases of the cell death process (45).

Although $P2X_7Rs$ were responsible for ATP-mediated necrotic cell swelling, ATP-induced cell death was not completely inhibited by siRNA (~50–60% of the control). The residual cell death is due to incomplete knock-down of $P2X_7Rs$ with siRNA and is also probably mediated by other P2X receptors that were not knocked down by the siRNA treatment. Actually, RT-PCR analysis has shown that SN4741 cells express $P2X_2R$, $P2X_4R$, and $P2X_5R$ (data not shown), indicating that multiple gene expression of the P2X family occurs in the SN4741 cells. Because other P2X receptors such as $P2X_4R$ and $P2X_6R$ have the potential to mediate cell death in various cells (*e.g.* mesangial cell, heart cells, and neuroblastoma cells) (46–48), it may be possible that other P2X receptors were partly involved here. We could not conclude that ATP-mediated necrotic cell swelling in SN4741 cells was solely dependent on $P2X_7R$. Nonetheless, our result showed that $P2X_7R$ was the main contributor to ATP-mediated cell death in SN4741 cells.

Unlike other P2X receptors, $P2X_7Rs$ require millimolar concentrations of ATP in the presence of divalent cations to achieve activation. This leads to the formation of nonselective cation channels and increased permeability to Ca^{2+} upon membrane depolarization (6). Because the balance between nucleotide release from cells and removal by extracellular enzymatic degradation determines extracellular ATP availability in the nervous system, the high concentrations of extracellular ATP to stimulate cytotoxic effects of $P2X_7Rs$ might not be reached *in vivo*. However, ATP can be actively released by regulated exocytosis in platelets, endothelial cells, and T cells and by traumatic cell lysis or passive leakage from damaged cells (49–51). On the other hand, The down-regulation of CD39 (ecto-ATP diphosphohydrolase) can also contribute to an accumulation of extracellular ATP (52). These events might result in an ATP-rich extracellular milieu reaching to millimolar ATP concentrations in the certain localized extracellular space (23).

Apart from excessive ATP accumulation, various mechanisms can also contribute to an neurodegenerative processes through $P2X_7Rs$. ATP itself participates in the up-regulation of $P2X_7Rs$ and initiates neuronal death in cerebellar granular neurons (53). In the pathological situation, the activity of $P2X_7Rs$ can be further complicated by the fact that the affinity of $P2X_7Rs$ for ATP increases as an inverse function of extracellular concentration of divalent cations (23, 54). Therefore, it is possible that the $P2X_7Rs$ in post-traumatic regions or in inflammatory regions are activated by lower concentrations of ATP than those observed *in vitro* (23). Collectively, these results support the notion that extracellular ATP can act in the surrounding degeneration site.

$P2X_7Rs$ have been proposed as potential therapeutic targets in various disorders of the nervous system including ischemia-reperfusion injury, Alzheimer disease, spinal cord injury, and neuropathic pain (5). In addition, dopaminergic cell death in the substantia nigra can directly lead to the progression of PD. Although *in vivo* the role of $P2X_7Rs$ in the progression of PD remains to be studied, our results indicate that degeneration of dopaminergic neurons caused by environmental or genetic factors can be accelerated by $P2X_7Rs$ activated by excess amounts of ATP released from damaged cells or activated astrocytes. A better understanding of the *in vivo* role of $P2X_7Rs$ in the process of neurodegeneration will help to treat the entire spectrum of neurodegenerative disease.

Acknowledgments—We sincerely thank Dr. James S. Willey and Dr. Ben J. Gu (University of Sydney) for providing us with the precious wild type and R307Q mutant $P2X_7R$ constructs. We also give our thanks to Dr. Se-Young Choi, Dr. Bo-hwa Choi, Dr. Dong-Chan Kim, and Sung-Jin Lee for technical assistance and helpful discussion.

REFERENCES

1. Moore, D. J., West, A. B., Dawson, V. L., and Dawson, T. M. (2005) *Ann. Rev. Neurosci.* **28,** 57–87
2. Whitton, P. S. (2007) *Br. J. Pharmacol.* **150,** 963–976
3. Dawson, T. M., and Dawson, V. L. (2003) *Science* **302,** 819–822
4. Morale, M. C., Serra, P. A., L'Episcopo, F., Tirolo, C., Caniglia, S., Testa, N., Gennuso, F., Giaquinta, G., Rocchitta, G., Desole, M. S., Miele, E., and Marchetti, B. (2006) *Neuroscience* **138,** 869–878
5. Le Feuvre, R., Brough, D., and Rothwell, N. (2002) *Eur. J. Pharmacol.* **447,** 261–269
6. Di Virgilio, F., Chiozzi, P., Ferrari, D., Falzoni, S., Sanz, J. M., Morelli, A., Torboli, M., Bolognesi, G., and Baricordi, O. R. (2001) *Blood* **97,** 587–600
7. Liang, L., and Schwiebert, E. M. (2005) *Am. J. Physiol.* **288,** C240–C242
8. Adriouch, S., Dox, C., Welge, V., Seman, M., Koch-Nolte, F., and Haag, F. (2002) *J. Immunol.* **169,** 4108–4112
9. Surprenant, A., Rassendren, F., Kawashima, E., North, R. A., and Buell, G. (1996) *Science* **272,** 735–738
10. Torres, G. E., Egan, T. M., and Voigt, M. M. (1999) *J. Biol. Chem.* **274,** 6653–6659
11. Inoue, K. (2002) *Glia* **40,** 156–163
12. Le Stunff, H., Auger, R., Kanellopoulos, J., and Raymond, M. N. (2004) *J. Biol. Chem.* **279,** 16918–16926
13. Ferrari, D., Los, M., Bauer, M. K., Vandenabeele, P., Wesselborg, S., and Schulze-Osthoff, K. (1999) *FEBS Lett.* **447,** 71–75
14. Wyllie, A. H., Kerr, J. F., and Currie, A. R. (1980) *Int. Rev. Cytol.* **68,** 251–306
15. Maeno, E., Ishizaki, Y., Kanaseki, T., Hazama, A., and Okada, Y. (2000) *Proc. Natl. Acad. Sci. U. S. A.* **97,** 9487–9492
16. Okada, Y., Maeno, E., Shimizu, T., Dezaki, K., Wang, J., and Morishima, S. (2001) *J. Physiol.* **532,** 3–16
17. Armstrong, J. N., Brust, T. B., Lewis, R. G., and MacVicar, B. A. (2002) *J. Neurosci.* **22,** 5938–5945
18. Duan, S., Anderson, C. M., Keung, E. C., Chen, Y., Chen, Y., and Swanson, R. A. (2003) *J. Neurosci.* **23,** 1320–1328
19. Deuchars, S. A., Atkinson, L., Brooke, R. E., Musa, H., Milligan, C. J., Batten, T. F., Buckley, N. J., Parson, S. H., and Deuchars, J. (2001) *J. Neurosci.* **21,** 7143–7152
20. Colomar, A., Marty, V., Medina, C., Combe, C., Parnet, P., and Amedee, T. (2003) *J. Biol. Chem.* **278,** 30732–30740
21. Virginio, C., MacKenzie, A., North, R. A., and Surprenant, A. (1999) *J. Physiol.* **519,** 335–346
22. Gu, B., Bendall, L. J., and Wiley, J. S. (1998) *Blood* **92,** 946–951
23. Wang, X., Arcuino, G., Takano, T., Lin, J., Peng, W. G., Wan, P., Li, P., Xu, Q., Liu, Q. S., Goldman, S. A., and Nedergaard, M. (2004) *Nat. Med.* **10,** 821–827
24. Son, J. H., Chun, H. S., Joh, T. H., Cho, S., Conti, B., and Lee, J. W. (1999) *J. Neurosci.* **19,** 10–20
25. Lee, H., Jun, D. J., Suh, B. C., Choi, B. H., Lee, J. H., Do, M. S., Suh, B. S., Ha, H., and Kim, K. T. (2005) *J. Biol. Chem.* **280,** 28556–28563
26. Di Virgilio, F., Fasolato, C., and Steinberg, T. H. (1988) *Biochem. J.* **256,** 959–963
27. Grynkiewicz, G., Poenie, M., and Tsien, R. Y. (1985) *J. Biol. Chem.* **260,** 3440–3450

28. Zholos, A., Beck, B., Sydorenko, V., Lemonnier, L., Bordat, P., Prevarskaya, N., and Skryma, R. (2005) *J. Gen. Physiol.* **125,** 197–211
29. Minta, A., and Tsien, R. Y. (1989) *J. Biol. Chem.* **264,** 19449–19457
30. Park, Y. S., Jun, D. J., Hur, E. M., Lee, S. K., Suh, B. S., and Kim, K. T. (2006) *Endocrinology* **147,** 1349–1356
31. Marcus, A. J., Broekman, M. J., Drosopoulos, J. H., Islam, N., Pinsky, D. J., Sesti, C., and Levi, R. (2003) *J. Pharmacol. Exp. Ther.* **305,** 9–16
32. Namgung, U., and Xia, Z. (2000) *J. Neurosci.* **20,** 6442–6451
33. Zeng, Y. S., and Xu, Z. C. (2000) *Neurosci. Res.* **37,** 113–125
34. Humphreys, B. D., Virginio, C., Surprenant, A., Rice, J., and Dubyak, G. R. (1998) *Mol. Pharmacol.* **54,** 22–32
35. Baraldi, P. G., Di Virgilio, F., and Romagnoli, R. (2004) *Curr. Top. Med. Chem.* **4,** 1707–1717
36. Virginio, C., Church, D., North, R. A., and Surprenant, A. (1997) *Neuropharmacology* **36,** 1285–1294
37. Mackenzie, A. B., Young, M. T., Adinolfi, E., and Surprenant, A. (2005) *J. Biol. Chem.* **280,** 33968–33976
38. Murgia, M., Hanau, S., Pizzo, P., Rippa, M., and Di Virgilio, F. (1993) *J. Biol. Chem.* **268,** 8199–8203
39. Gu, B. J., Sluyter, R., Skarratt, K. K., Shemon, A. N., Dao-Ung, L. P., Fuller, S. J., Barden, J. A., Clarke, A. L., Petrou, S., and Wiley, J. S. (2004) *J. Biol. Chem.* **279,** 31287–31295
40. Wiley, J. S., Dao-Ung, L. P., Li, C., Shemon, A. N., Gu, B. J., Smart, M. L., Fuller, S. J., Barden, J. A., Petrou, S., and Sluyter, R. (2003) *J. Biol. Chem.* **278,** 17108–17113
41. Gu, B. J., Zhang, W., Worthington, R. A., Sluyter, R., Dao-Ung, P., Petrou, S., Barden, J. A., and Wiley, J. S. (2001) *J. Biol. Chem.* **276,** 11135–11142
42. Sluyter, R., Shemon, A. N., and Wiley, J. S. (2004) *J. Immunol.* **172,** 3399–3405
43. Anderson, C. M., and Nedergaard, M. (2006) *Trends Neurosci.* **29,** 257–262
44. Sperlagh, B., Vizi, E. S., Wirkner, K., and Illes, P. (2006) *Prog. Neurobiol.* **78,** 327–346
45. Formigli, L., Papucci, L., Tani, A., Schiavone, N., Tempestini, A., Orlandini, G. E., Capaccioli, S., and Orlandini, S. Z. (2000) *J. Cell Physiol.* **182,** 41–49
46. Solini, A., Santini, E., Chimenti, D., Chiozzi, P., Pratesi, F., Cuccato, S., Falzoni, S., Lupi, R., Ferrannini, E., Pugliese, G., and Virgilio, F. D. (2007) *Am. J. Physiol.* **292,** F1537–F1547
47. Banfi, C., Ferrario, S., De Vincenti, O., Ceruti, S., Fumagalli, M., Mazzola, A. N. D. A., Volonte, C., Fratto, P., Vitali, E., Burnstock, G., Beltrami, E., Parolari, A., Polvani, G., Biglioli, P., Tremoli, E., and Abbracchio, M. P. (2005) *J. Mol. Cell. Cardiol.* **39,** 929–939
48. Cavaliere, F., Nestola, V., Amadio, S., D'Ambrosi, N., Angelini, D. F., Sancesario, G., Bernardi, G., and Volonte, C. (2005) *Neurobiol. Dis.* **18,** 100–109
49. Beigi, R., Kobatake, E., Aizawa, M., and Dubyak, G. R. (1999) *Am. J. Physiol.* **276,** C267–C278
50. Filippini, A., Taffs, R. E., and Sitkovsky, M. V. (1990) *Proc. Natl. Acad. Sci. U. S. A.* **87,** 8267–8271
51. Pearson, J. D., and Gordon, J. L. (1979) *Nature* **281,** 384–386
52. Robson, S. C., Kaczmarek, E., Siegel, J. B., Candinas, D., Koziak, K., Millan, M., Hancock, W. W., and Bach, F. H. (1997) *J. Exp. Med.* **185,** 153–163
53. Amadio, S., D'Ambrosi, N., Cavaliere, F., Murra, B., Sancesario, G., Bernardi, G., Burnstock, G., and Volonte, C. (2002) *Neuropharmacology* **42,** 489–501
54. North, R. A. (2002) *Physiol. Rev.* **82,** 1013–1067

Extracellular ATP Mediates Necrotic Cell Swelling in SN4741 Dopaminergic Neurons through P2X $_7$ Receptors

Dong-Jae Jun, Jaeyoon Kim, Sang-Yong Jung, Ran Song, Ji-Hyun Noh, Yong-Soo Park, Sung-Ho Ryu, Joung-Hun Kim, Young-Yun Kong, Jun-Mo Chung and Kyong-Tai Kim

J. Biol. Chem. 2007, 282:37350-37358.
doi: 10.1074/jbc.M707915200 originally published online October 25, 2007
